THE JOURNAL OF PHYSICAL CHEMISTRY C

Article

pubs.acs.org/JPCC

Unusual Weak Interparticle Distance Dependence in Raman Enhancement from Nanoparticle Dimers

Zhaoxia Qian,[†] Chen Li,[†] Zahra Fakhraai,*[,†] and So-Jung Park*[,‡]

[†]Department of Chemistry, University of Pennsylvania, Philadelphia, Pennsylvania 19104, United States

[‡]Department of Chemistry & Nano Science, Ewha Womans University, 11-1, Daehyeon-dong, Seodaemun-gu, Seoul, South Korea

Supporting Information

ABSTRACT: Here, we report surprisingly weak distance dependence in Raman enhancement from a raspberry-like gold nanoparticle termed raspberry-MM. A raspberry-MM is composed of closely packed gold nanobeads assembled on a polymer core. Due to the abundant "built-in" hot spots between adjacent gold nanobeads, bright and uniform Raman signals were observed from isolated single raspberry-MMs. Interestingly, dimers of raspberry-MMs also showed highly reproducible Raman signals, indicating that the dimer SERS signal is not strongly dependent on the nanoparticle separation. Finite-difference time-domain (FDTD) modeling shows that a strong hot spot is created at the dimer-gap, as expected. However, since there are many more built-in hot spots in each raspberry-MM, the contribution of the dimer-gap hot spot to the total Raman enhancement remains low even for 2 nm separation, which explains the observed weak distance dependence. This result is in stark contrast with many previous SERS studies on nanoparticle dimers and clusters, and provides an important guideline on how to design bright and highly reproducible Raman substrates.

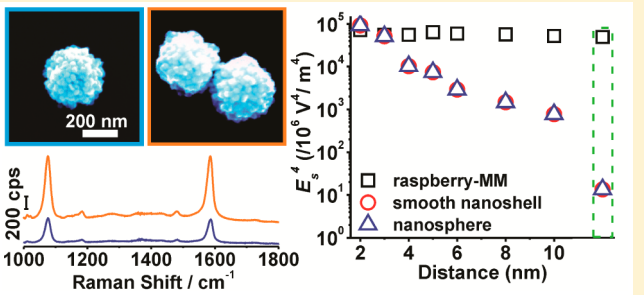

Highly enhanced local field or "hot spots" can be created at the gap between two closely spaced metal nanoparticles.[1,2] These hot spots make it possible to detect Raman signals at extremely low concentrations[3] or even at the single molecule level.[4] Numerous studies have shown that the Raman enhancement from nanoparticle dimers[2,5,6] depends highly on the separation between two particles. Therefore, the ability to control the interparticle distance with a nanometer scale precision is critical for practical applications of hot-spot-based surface enhanced Raman spectroscopy (SERS).

While tremendous efforts have been put into preparing nanoparticle dimers with controlled interparticle distances through the bottom-up self-assembly[7−10] or top-down lithographic methods,[11,12] it still remains a significant challenge to create such nanostructures in a cost-effective way. In addition, the strong SERS signal from nanoparticle dimers can result in false positive signals in sensing applications of SERS due to the accidental aggregation of nanoparticles. Therefore, a bright and uniform particle whose dimers exhibit weak distance dependence constitutes an ideal design of SERS substrate.

Here, we report surprisingly weak distance dependence in SERS from raspberry-like gold nanoparticles, which were termed raspberry-like metamolecules (raspberry-MMs) in our previous report.[13] Raspberry-MMs, which are composed of closely packed gold nanobeads assembled on a polymer core, exhibit a bright and highly reproducible SERS signal at the single particle level due to the large number of "built-in" hot spots in a single raspberry-MM. Interestingly, dimers of raspberry-MMs also showed very small variations in SERS intensities. This result is in stark contrast with many other metal nanostructures studied in the past, where strong distance dependence and extremely large intensity variations were usually observed.[6−8,12] Finite-difference time-domain (FDTD) simulations were carried out to quantitatively explain the weak distance dependence shown in raspberry-MM dimers. To the best of our knowledge, this is the first example showing weak distance dependence in SERS. We believe that the findings in this study provide an important guideline in designing SERS substrates exhibiting bright and reproducible signals.

EXPERIMENTAL METHODS

Materials and Instrumentation. Benzyl dimethyl hexadecyl ammonium chloride (BDAC), chloroauric acid ($HAuCl_4$), sodium borohydride ($NaBH_4$), silver nitrate ($AgNO_3$), ascorbic acid, and 4-mercaptobenzoic acid (4-MBA) were purchased from Sigma-Aldrich. Ammonium hydroxide was purchased from Fisher Scientific. Carboxylate-modified FluoSpheres (100 nm, 2 wt % solids; 200 nm diameter, 4 wt % solids) were purchased from Invitrogen, and their average diameters were determined to be 94.5 ± 7.2 nm and 184.2 ± 9.4 nm, respectively, by transmission electron microscope (TEM) measurements. TEM images were taken

Received: September 26, 2015
Revised: October 29, 2015

DOI: 10.1021/acs.jpcc.5b09396
J. Phys. Chem. C XXXX, XXX, XXX−XXX

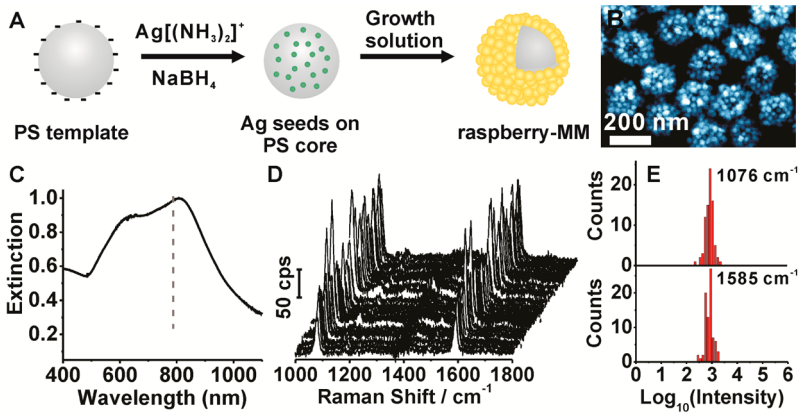

Figure 1. (A) Schematic description of the synthetic procedure of raspberry-MMs. The gray, blue, and yellow spheres represent the PS template, Ag seed particles, and gold nanobeads, respectively. (B) An SEM image of typical raspberry-MMs synthesized by the seed-mediated method.[13] For this particular synthesis, 35 μL of seed solution was mixed with 10 mL of growth solution. The size parameters of the raspberry-MMs shown in this image are PS core diameter (D_{core}) = 94.5 ± 7.2 nm, average number of beads (N_{bead}) = 98 ± 10, the diameter of the bead (D_{bead}) = 32.6 ± 7.6 nm, and the average diameter of the raspberry-MM (D_{RMM}) = 198 ± 14 nm. (C) The extinction spectrum of typical raspberry-MMs shown in part B. The gray dashed line indicates the excitation wavelength (785 nm) used for Raman measurements. (D) Raman spectra of 4-MBA from 82 single raspberry-MMs. The average intensity at 1076 and 1585 cm^{-1} were 91 ± 33 counts per seconds (cps) and 85 ± 30 cps, respectively. (E) Histograms showing the distribution of SERS intensities at 1076 cm^{-1} (top) and 1585 cm^{-1} (bottom).

with a JEOL 2100 operating at 200 kV accelerating voltage. Scanning electron microscope (SEM) images were obtained using Quanta 600 FEG Mark II at 30 kV accelerating voltage. Extinction spectra were measured with an Agilent 8453 UV−vis spectrophotometer.

Synthesis of Raspberry-like Metamolecules (Raspberry-MMs). The raspberry-MMs were synthesized by a templated surfactant-assisted seed growth method.[13] Typically, carboxylate-modified FluoSpheres (100 or 200 nm diameter, 100 μL) were mixed with an aqueous solution of $Ag(NH_3)_2^+$ (0.01 M, 1 mL) for 30 min. Then the solution was centrifuged at 18 000 rpm for 30 min, and the supernatant was replaced with purified water. The same washing procedure was repeated one more time, and the precipitates were redispersed in 500 μL of water, followed by quick injection of freshly prepared $NaBH_4$ (0.01 M, 100 μL) solution upon vigorous vortexing for 10 s. After aging at room temperature overnight, the solution was centrifuged at 18 000 rpm for 30 min and redispersed in 5 mL of water.

The growth solution was prepared by mixing aqueous solutions of BDAC (0.1 M, 10 mL), $HAuCl_4$ (0.01 M, 421 μL), $AgNO_3$ (0.01 M, 64 μL), and ascorbic acid (0.1 M, 67 μL). In a typical synthesis, 20−70 μL of seed solution was added to the growth solution, followed by a gentle shaking for a few seconds. Red color started to develop after approximately 10 min, and the reaction was completed in 2 h. The raspberry-MMs were centrifuged at 4000 rpm for 10 min to remove excess BDAC. The same centrifugation procedure was repeated one more time, and the raspberry-MMs were redispersed in 0.5 mL of water for further characterizations.

Raman Measurements. For single particle or dimer measurements, 5 μL of raspberry-MM solution was placed on a piranha-cleaned silicon wafer; the wafer was then placed in a homemade humidity chamber for 30 s, which was then rinsed with water and dried with nitrogen gas. This procedure results in many isolated raspberry-MMs and some accidently formed clusters (dimers, trimers, etc.) of raspberry-MMs on the substrate. The analyte molecule, 4-mercaptobenzoic acid (4-MBA), was deposited onto raspberry-MMs by submerging the silicon wafer into a 2 mM ethanolic solution of 4-MBA for 12 h. The wafer was rinsed with water and dried under the flow of nitrogen gas. Raman measurements were performed on a VIS Raman Microspectrometer (Renishaw RM1000). A beam of 785 nm from a diode laser (Class IIIb lasers, 500 mW) was sent through a 100 cm^{-1} cutoff notch filter and focused onto the sample via a 100× objective (Leica Germany, NA = 0.90). Typical laser power density and acquisition time for SERS measurements were 2.63 × 10^3 W/cm^2 and 10 s, respectively. Raman samples were imaged by SEM to ensure that only raspberry-MM monomers and dimers were included in each analysis.

Finite-Difference Time-Domain (FDTD) Simulations. Finite-difference time-domain (FDTD) simulations were performed using Lumerical Solutions, Inc. FDTD package Version 8.7 and 8.11. Details of our models and FDTD simulations were described in our previous publication.[13] The model created using a molecular dynamics simulation[13] is composed of 800 gold nanobeads closely packed onto a spherical PS core with an overall diameter of 184 nm. Each gold nanobead is made of a 13 nm spherical gold core and a 1 nm PS shell. The PS shell was used to mimic the BDAC surfactant layer on the gold surface and to keep the gold particles physically isolated. The raspberry-MM dimers were generated by placing two identical particles separated at a designated distance (2−50 nm). A broadband total-field scatter-field (TFSF) pulse was injected into the rectangular simulation region enclosing the modeled structure, and a perfectly matched layer (PML) absorbing boundary condition was applied. The electric field inside of the simulation region was recorded, and its sum over all space was calculated. The near field intensity distribution was calculated using the squared norm of the complex field vectors. The Raman enhancement at each position was calculated by multiplying the field intensity at the excitation frequency with that at the Stokes frequency.

RESULTS AND DISCUSSION

Raman Enhancement from Single Raspberry-MMs. A series of raspberry-MMs were synthesized by the templated surfactant-assisted seed-mediated method (Figure 1A) described in our previous publication.[13] A raspberry-MM is

DOI: 10.1021/acs.jpcc.5b09396
J. Phys. Chem. C XXXX, XXX, XXX−XXX

composed of a large number of gold nanobeads assembled on a spherical polystyrene (PS) template.[13] We have demonstrated in our previous study that gold nanobeads composing raspberry-MMs are physically isolated with about a couple of nanometers separation.[13] Figures1B and 1C show an SEM image and the extinction spectrum of a typical raspberry-MM sample composed of a PS core with a diameter of 94.5 ±7.2 nm and gold nanobeads with an average diameter of 32.6 ± 7.6 nm. As reported in our previous publication,[13] the broad extinction spectrum of raspberry-MMs shown in Figure 1C indicates that raspberry-MMs are composed of closely packed, intact gold nanobeads. These structural characteristics suggest that raspberry-MMs should act as efficient SERS substrates as they contain many "built-in" hot spots between individual gold nanobeads (termed built-in hot spots hereafter).

Single particle SERS measurements were carried out on raspberry-MMs using 4-mercaptobenzoic acid (4-MBA) as an analyte. Figure 1D presents single particle SERS spectra collected from 82 different raspberry-MMs, which show two major Raman peaks characteristic of 4-MBA; the two peaks at 1076 and 1585 cm^{-1} were assigned to the combination band of the phenyl ring-breathing and C−S stretching modes and the phenyl ring C−C stretching mode, respectively.[14] Importantly, without exception, all examined raspberry-MMs exhibited intense Raman signals at the single particle level. The bright Raman signals from single raspberry-MMs are attributed to the abundant built-in hot spots in a single raspberry-MM (Figure S1). For comparison, simple gold nanoshells composed of a 120 nm SiO_2 core and a 15 nm thick gold shell showed more than an order of magnitude weaker Raman intensity under the same experimental conditions (Figure S2).

Importantly, single particle Raman scattering signals from raspberry-MMs were narrowly distributed within an order of magnitude (Figure 1E). This is a significant advantage over most other hot-spot-based SERS substrates showing extremely broad intensity distributions.[2,15] As mentioned above, Raman enhancement of reported nanoparticle clusters depends highly on the exact local structure, and the intensity varies many orders of magnitude from one cluster to another.[15] Recently, there have been a few reports on hot-spot-based SERS substrates showing both high reproducibility and enhancement at the single particle level.[16,17] For example, Lim et al. reported a DNA-based synthesis of metal nanoparticles with 1 nm interior gap, where 90% of individual nanoparticles exhibited uniform Raman scattering intensities.[16] In the raspberry-MMs reported here, virtually all measured particles showed strong Raman signal with narrow intensity distribution owing to the large number of built-in hot spots.

The strength of Raman enhancement on raspberry-MMs can be controlled by varying their structure parameters (Figure 2). A series of raspberry-MMs with different structure parameters (Figure 2A−D) were synthesized for single particle SERS measurements. When the overall diameter of the raspberry-MM was increased from 164 nm (Figure 2A) to 228 nm (Figure 2B) by increasing the size of gold nanobeads at a fixed core diameter (94.5 nm) and the number of nanobeads (~100), the Raman intensity at 1076 cm^{-1} increased by a factor of 4 presumably due to the stronger hot spots created between larger nanobeads (Figure S3). When the diameter of the raspberry-MMs was further increased to 337 nm by increasing the size of the PS core (184 nm) and the number of beads (>400) (Figure 2C), the Raman intensity increased further (Figure 2E), primarily due to the increased number of built-in

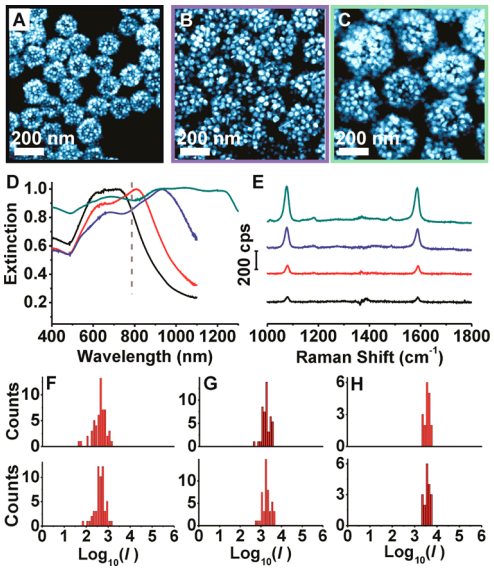

Figure 2. (A−C) SEM images of different size raspberry-MMs used for single particle SERS measurements. The size parameters of these raspberry-MMs are (A) D_{core} = 94.5 ± 7.2 nm, N_{bead} = 93 ± 10, D_{bead} = 23.6 ± 5.6 nm, D_{RMM} = 164 ± 14 nm; (B) D_{core} = 94.5 ± 7.2 nm, N_{bead} = 97 ± 15, D_{bead} = 38.8 ± 10.8 nm, D_{RMM} = 228 ± 23 nm; (C) D_{core} = 184 ± 9 nm, N_{bead} > 400, D_{bead} = 29.6 ± 10.0 nm, D_{RMM} = 337 ± 27 nm. For the syntheses, 10 mL of growth solution was mixed with 70 μL (A), 20 μL (B), or 35 μL (C) of seed solution. (D) Extinction spectra of raspberry-MMs are shown in (A) black, (B) blue, and (C) dark cyan. The extinction spectrum of raspberry-MMs shown in Figure 1B (red) was also plotted for comparison. The gray dashed line indicates the excitation wavelength (785 nm). (E) Averaged spectra of single particle measurement for raspberry-MMs shown in part A (black), Figure 1B (red), part C (blue), and part D (dark cyan). The average intensities at 1076 and 1585 cm^{-1} were 56 ± 34 and 49 ± 27 cps for part A, 220 ± 133 and 199 ± 110 cps for part B, and 383 ± 98 and 345 ± 111 cps for part C, respectively. (F−H) Intensity histograms for raspberry-MMs shown in part A (F), part B (G), and part C (H) at 1076 cm^{-1} (top) and 1585 cm^{-1} (bottom).

hot spots. The peak positions of extinction spectra are not correlated with the Raman intensities of different sized raspberry-MMs (Figure 2D), consistent with previous reports on hot-spot-based SERS.[2,18] Note that all measurements from different sized raspberry-MMs show narrow distributions in Raman intensities (Figure 2F−H).

Raman Enhancement from Raspberry-MM Dimers. Raman spectra were collected from raspberry-MM dimers to investigate the distance dependence of SERS enhancement (Figure 3). Figure 3A presents SEM images of raspberry-MM dimers used for the measurements. Since these dimers were randomly formed during drop-casting, the interparticle distance between two raspberry-MMs was not controlled. Nonetheless, most dimers presented in Figure 3A are closely spaced except the one highlighted with a red box (Figure 3A). Figure 3B,C shows measured SERS spectra taken from raspberry-MM dimers (Figure 3B) and individual raspberry-MMs (Figure 3C). The peak intensities from the measurements are plotted in Figure 3D for easy comparison. It is interesting to find that the average Raman intensity from the raspberry-MM dimers is only 2.8 times higher than that of single raspberry-MMs. This result is different from SERS measurements on other types of nanoparticles.[2,6−8,19] It is well-known that, for simple nanoparticles such as nanospheres and rods, the Raman intensity

DOI: 10.1021/acs.jpcc.5b09396
J. Phys. Chem. C XXXX, XXX, XXX−XXX

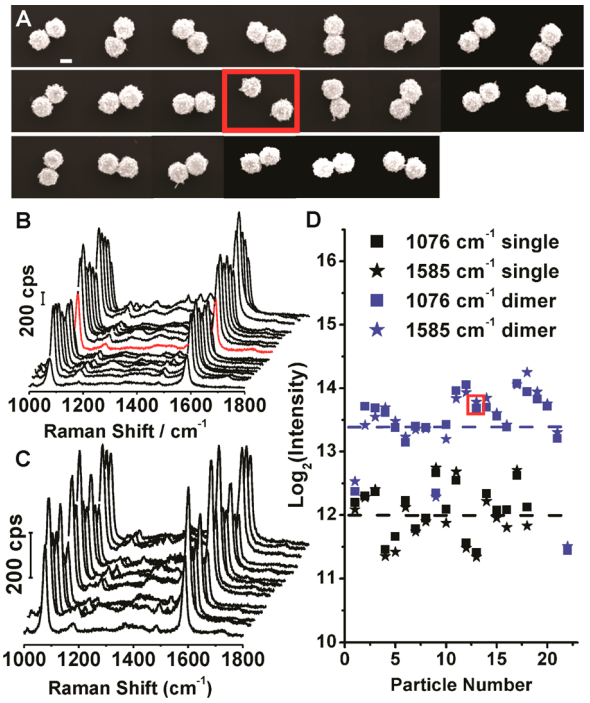

Figure 3. (A) SEM images of 20 two raspberry-MM (D_{core} = 184 ± 9 nm, N_{bead} > 400, D_{bead} = 29.6 ± 10.0 nm, D_{RMM} = 337 ± 27 nm) dimers with random interparticle distances. Scale bar is 200 nm. The separation between the two raspberry-MMs encased in the red box is approximately 290 nm. (B) SERS data from the raspberry-MM dimers shown in part A; the average Raman intensities at 1076 and 1585 cm^{-1} were 1169 ± 374 and 1182 ± 390 cps, respectively. The spectrum highlighted in red corresponds to the raspberry-MM dimer encased in the red box in part A. (C) Single particle SERS data from 18 different raspberry-MMs. The average Raman intensities at 1076 and 1585 cm^{-1} were 383 ± 98 cps and 345 ± 111 cps, respectively. (D) Raman intensity distributions of single raspberry-MMs and raspberry-MM dimers at 1076 and 1585 cm^{-1}. The dashed lines indicate the average signal intensity at 1076 cm^{-1}.

dramatically increases with dimerization.[7,8,19] For example, the SERS signal from 50 nm gold particles was observed to increase about 100 times upon dimerization.[7] Theoretical calculations predict that the Raman enhancement of gold nanoparticle dimers can be up to 3 orders of magnitude larger than the enhancement observed from single nanoparticles.[5] For more complex nanostructures, Liang et al.[6] found that the SERS intensity from flower-like silver mesoparticle dimers was 10–100 times higher than that of single mesoparticles. To the best of our knowledge, the results described here are the first to show that the Raman enhancement does not increase substantially with dimerization. Consequently, the dimer Raman intensity shows a narrow distribution. Note that the two particles separated by 290 nm (encased in a red box, Figure 3) showed peak intensities similar to those from other dimers with small interparticle distances. Also note that the reproducibility of the dimer data is as good as that of single particle data with similar levels of intensity variations (Figure 3D). These results indicate that raspberry-MMs exhibit weak distance dependence in Raman enhancement.

Origin of Reproducible Raman Enhancement from Single Raspberry-MMs. Finite-difference time-domain (FDTD) simulations were performed to calculate the electric field distribution in raspberry-MM monomers. A raspberry-MM model composed of 800 gold beads closely packed on a 184 nm spherical PS core (Figure 4A) was used to mimic the experimental structure of a single raspberry-MM. In this model, gold nanobeads had an average end-to-end interparticle distance of 1.7 ± 0.1 nm (Figure S4), which is similar to the expected thickness of BDAC layer surrounding the nanobeads. A more detailed description on the model and the setup of the simulation is provided in our earlier publication.[13] As previously reported,[13] the calculated far field extinction spectra of this model reproduce the general features of the experimental spectra, showing the validity of the model structure (Figure S4). FDTD simulations for the same raspberry-MM models were used here to estimate the near field enhancement and to calculate the Raman enhancement.

First, the electromagnetic field intensities (E^2) at the excitation wavelength (785 nm, Figure 4B) and the Stokes wavelength (860 nm, Figure S5) were calculated for an individual raspberry-MM. The field map presented in Figure 4B (top) shows that the electric field in individual raspberry-MMs is mainly confined in built-in hot spots (Figure S1). The intensity at these built-in hot spots varies at different locations within the raspberry-MM (Figure 4B, top) due to the variations

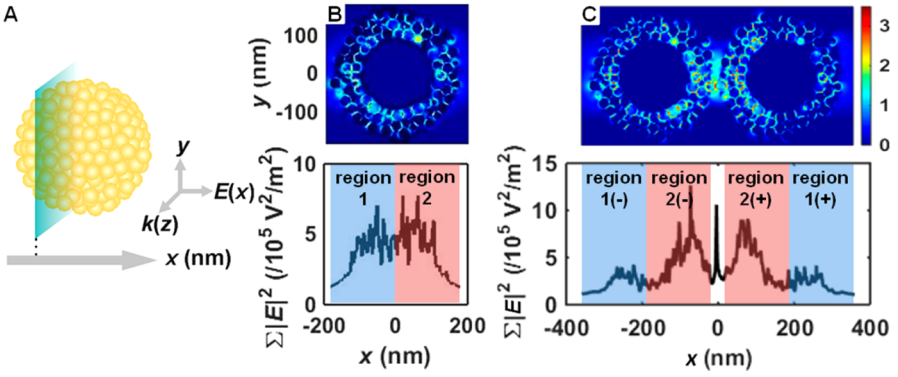

Figure 4. (A) Modeled raspberry-MM (D_{core} = 184 nm, N_{bead} = 800, D_{bead} = 28 nm, D_{RMM} = 340 nm) and schematic description of how it was sliced in Cartesian coordinate system. The blue slab is perpendicular to the x axis and has a thickness of 1.2 nm (mesh size used for the FDTD simulations). (B) Top: Electric field intensity (E^2) map for the z = 0 plane of a single raspberry-MM. Bottom: E^2 summed over the yz slab indicated in (A) (ΣE^2) plotted along the x direction. (C) Electric field intensity distribution (top) and ΣE^2 profile (bottom) for a raspberry-MM dimer (2 nm separation). The incident light is polarized along the x axis and propagates along the z axis. All calculations presented here are for 785 nm. The color bar is in a logarithmic scale.

DOI: 10.1021/acs.jpcc.5b09396
J. Phys. Chem. C XXXX, XXX, XXX–XXX

in the gap size (Figure S4). The spatial intensity distribution of the built-in hot spots also varies from one raspberry-MM to another, depending on their exact structures. However, the total electric field intensity of individual raspberry-MMs does not change much from one raspberry-MM to another due to the averaging effect over the large number of built-in hot spots in single raspberry-MMs (Figure S6), which is consistent with our experimental data.

Origin of Weak Distance Dependence of Raman Enhancement of Raspberry-MM Dimers. In order to understand why the Raman enhancement does not increase substantially with dimerization, electric field distributions were calculated for raspberry-MM dimers with varying interparticle distances. Figure 4C presents the electric field intensity map (E^2) of raspberry-MM dimers placed at 2 nm separation for the excitation wavelength (785 nm). When the incident light is polarized along the dimer axis, a new hot spot is created at the gap between the two raspberry-MMs (named dimer-gap hot spots hereafter) as evidenced by the peak at x = 0 nm in the electric field intensity profile (Figure 4C, bottom). The intensity of the dimer-gap hot spot is higher than the intensities at most built-in hot spots (Figure 4C, top). It is also worth noting that the electric field intensity distribution on raspberry-MMs changes with dimerization; the field intensity increases in region 2 (close to the dimer-gap), and decreases in region 1 (away from the dimer-gap) (Figure 4C). Similar trends were observed for the Stokes wavelength (860 nm) (Figure S5). The changes in the field intensity distribution upon dimerization indicate that there is plasmonic coupling between adjacent raspberry-MMs.[20] Similar results were observed for raspberry-MM dimers for other separation distances (Table S1, Figures S7–S10). This result is consistent with the observation that raspberry-MM monomers and dimers show different far field spectra (Figures S11 and S12). We believe that this field intensity redistribution contributes to the slight increase in Raman enhancement with dimerization (*vide infra*). As expected, the plasmonic coupling between adjacent raspberry-MMs is much weaker for the polarization direction perpendicular to the dimer axis (Figure S13); no strong dimer-gap hot spot is created (Figure S13C–F), and the field intensity distribution remains about the same before and after dimerization (Figure S13).

The Raman enhancements (E_s^4, E_t^4) of the raspberry-MM monomer and dimer models were calculated by integrating the product of electric field intensity (E^2) at 785 nm (excitation wavelength) and that at 860 nm (Stokes wavelength). The E_s^4 refers to the E^4 added up from the surface of the PS core to the surface of the raspberry-MMs, while E_t^4 refers to the total E^4 inside of the entire simulation box excluding the PS core region (see Table S5). The two values are close given that the electric field enhancement outside of the raspberry-MMs quickly drops to zero, but E_s^4 is a slightly better representation of the experimental SERS data as the analyte molecules are only on the surface of nanoparticles.

The calculated Raman enhancement E_s^4 agrees well with the experimental data. When the incident light is polarized along the dimer axis, the E_s^4 of the raspberry-MM dimer with a 2 nm separation is calculated to be 3.4 times of the monomer value (Table S6). For the polarization direction perpendicular to the dimer axis, the Raman enhancement is calculated to be similar to that from an individual raspberry-MM (Table S6). The experimental ratio between the Raman intensities for dimers and monomers was determined to be 2.8, which is in-between the calculated field enhancement ratios for the two different polarization direction (3.4 and 1.3, Table S6). Considering that nonpolarized light was used for the experimental Raman measurements, the calculated values are in good agreement with experimental data.

In order to understand the effect of the dimer-gap hot spot on the total Raman enhancement, the Raman enhancement (E^4) maps and ΣE^4 profiles were obtained for a raspberry-MM monomer and a dimer and presented in Figure 5. The data in

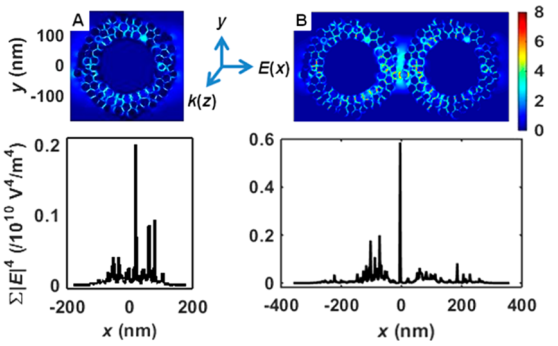

Figure 5. (A) Raman enhancement (E^4) map for the z = 0 plane (top) and ΣE^4 profile (bottom) of a raspberry-MM monomer. (B) Raman enhancement (E^4) map for the z = 0 plane (top) and ΣE^4 profile (bottom) of a raspberry-MM dimer (2 nm separation). The incident light is polarized along the x axis and propagates along the z axis. The color bar is in a logarithmic scale.

Figure 5B show that the Raman enhancement from the dimer-gap hot spot (E_h^4) is at least an order of magnitude higher than that from an average built-in hot spot for 2 nm separation. The E_h^4 values were calculated at varying interparticle distances to investigate the distance dependence (Figure 6A, black square).

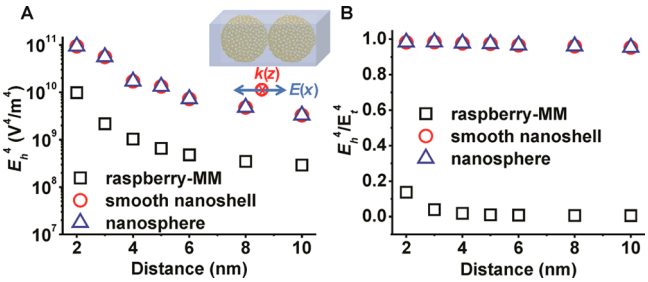

Figure 6. (A) Distance-dependent E_h^4 of the raspberry-MM dimers (black □), smooth nanoshell (184 nm PS core diameter, 77 nm shell thickness) dimers (red ○), and Au nanosphere (338 nm diameter) dimers (blue △). (B) The ratio between the Raman enhancement at the dimer-gap hot spots (E_h^4) and the total E^4 (E_t^4) for raspberry-MMs (black □), smooth PS@Au nanoshells (red ○), and nanospheres (blue △) as a function of separation distances. The incident light is polarized along the x axis and propagates along the z axis, as shown in the inset of part A. See Tables S2–S4 for specific geometric definition of the dimer-gap hot spot and Table S5 for E_t^4.

As expected, the E_h^4 decreases with increasing the separation (Figure 6A, black squares, Table S2). Similar distance dependence was observed for smooth nanoshell and nanosphere dimers (Figure 6A, red circles and blue triangles, respectively, Tables S3 and S4), consistent with previous reports.

DOI: 10.1021/acs.jpcc.5b09396
J. Phys. Chem. C XXXX, XXX, XXX–XXX

However, since there are many built-in hot spots in a raspberry-MM, the contribution of the dimer-gap hot spot to the total enhancement (E_h^4/E_t^4) is only 14% even for raspberry-MM dimers separated by 2 nm (Figure 6B). This characteristic distinguishes raspberry-MMs from many previously studied systems which showed that the majority of the Raman enhancement of nanoparticle dimers comes from the hot spot in the gap.[5,6,8] For example, E_h^4/E_t^4 is calculated to be over 95% for both smooth PS@Au nanoshell dimers and Au nanosphere dimers at the same separation (Figure 6B). In the simple nanostructures of smooth nanoshells and spheres, the majority of Raman enhancement comes from the dimer-gap hot spot over a range of interparticle distances (Figure 6B, red ○ and blue △, respectively, Tables S3 and S4, and Figures S18 and S19). For raspberry-MMs, the low E_h^4/E_t^4 value is further reduced with increasing the interparticle distance, and it stays low over a wide distance range (Figure 6B, black □, Table S2, and Figures S14–S17).

Consequently, for smooth nanoshells and nanospheres where the dimer-gap hot spot makes the major contribution to the Raman enhancement, E_s^4 (Raman enhancement) falls quickly with increasing interparticle distances (Figure 7). It is well-documented that the electromagnetic field intensity and Raman enhancement from nanoparticle dimers decay rapidly with increasing interparticle distances.[21] For example, Lee et al. reported that the Raman enhancement of face-to-face silver nanocube dimers decreased by 3 orders of magnitude when the distance increases from 3 to 10 nm both experimentally and via simulation.[12] Stewart et al. observed that the Raman enhancement of gold nanorod dimers decreased by a factor of 10 when the end-to-end distance increased from 2 to 9 nm.[19] Our simulation data for nanoshells and nanospheres (Figure 7 and Figure S20) are consistent with the previous reports.[21] For raspberry-MMs, the Raman enhancement does not change substantially with interparticle distance (Figures 7 and S20), as the dominant Raman enhancement comes from the large number of built-in hot spots rather than the dimer-gap hot spot. This simulation result explains the experimental observation that the Raman enhancement from raspberry-MMs is fairly uniform even for dimers and the Raman intensity does not increase substantially with dimerization.

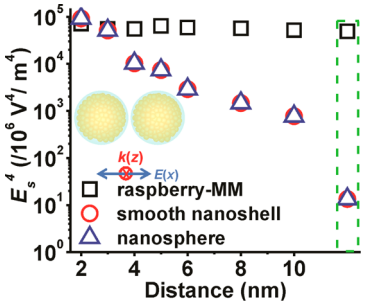

Figure 7. Raman enhancement (E_s^4) of raspberry-MM dimers (black □), smooth PS@Au nanoshell dimers (red ○), and Au nanosphere dimers (blue △) at varying separation distances. The data points encased in the green box represent the two times of E_s^4 for the corresponding single particle. As depicted in the inset graphic, E_s^4 was calculated by adding up E^4 inside the shell volume (inside the sky blue sphere and outside the PS core). The incident light is polarized along the x axis and propagates along the z direction, as shown in the inset.

CONCLUSION

In summary, we report the surprisingly weak distance dependence in SERS from raspberry-like gold particles termed raspberry-MMs. SERS measurements carried out for 4-MBA immobilized on raspberry-MMs showed a strong and highly reproducible Raman signal at the single particle level, which was attributed to the large number of built-in hot spots at the junctions between many closely spaced gold nanobeads in each raspberry-MM. Surprisingly, the Raman intensity did not substantially increase with dimerization of raspberry-MMs, and the accidentally formed dimers showed little variations in Raman intensity. FDTD simulations showed that although a hot spot is created at the gap between two raspberry-MMs, the majority of Raman enhancement comes from the large number of built-in hot spots. The simulation data explain the experimentally observed weak distance dependence in SERS from raspberry-MMs. The weak distance dependence found here contrast with many previous reports[6−8] showing orders of magnitude increase in SERS intensity upon dimer formation. In addition, unlike previous studies[2,12] showing extremely large variations in Raman intensities from nanoparticle junctions, raspberry-MM dimers studied here showed uniform intensities distributed within the same order of magnitude. This unique characteristic relieves the complications associated with the accidental cluster formation in SERS-based sensing applications. Indeed, the findings in this study provide an important guideline in designing SERS substrates exhibiting bright and reproducible signals.

ASSOCIATED CONTENT

Supporting Information

The Supporting Information is available free of charge on the ACS Publications website at DOI: 10.1021/acs.jpcc.5b09396.

Additional TEM images, and electromagnetic field intensity distributions of single raspberry-MM, raspberry-MM dimers, and smooth nanoshells (PDF)

AUTHOR INFORMATION

Corresponding Authors

*E-mail: fakhraai@sas.upenn.edu.
*E-mail: sojungpark@ewha.ac.kr.

Notes

The authors declare no competing financial interest.

ACKNOWLEDGMENTS

S.-J.P. acknowledges the financial support from the National Research Foundation of Korea grant funded by the Korea government (MSIP) (NRF-2015R1A2A2A01003528) and the Air Force Office of Scientific Research. TEM and SEM measurements were carried out at the Electron Microscopy Resource Laboratory and the Singh Center for Nanotechnology in University of Pennsylvania. Z.F. acknowledges startup funding from the University of Pennsylvania. The authors acknowledge Dr. Simon P. Hastings for his constructive suggestions on plotting the field distribution lines.

REFERENCES

(1) Li, W.; Camargo, P. H. C.; Lu, X.; Xia, Y. Dimers of Silver Nanospheres: Facile Synthesis and Their Use as Hot Spots for Surface-Enhanced Raman Scattering. *Nano Lett.* **2009**, *9*, 485−490.
(2) Wustholz, K. L.; Henry, A.-I.; McMahon, J. M.; Freeman, R. G.; Valley, N.; Piotti, M. E.; Natan, M. J.; Schatz, G. C.; Duyne, R. P. V.

DOI: 10.1021/acs.jpcc.5b09396
J. Phys. Chem. C XXXX, XXX, XXX−XXX

Structure−Activity Relationships in Gold Nanoparticle Dimers and Trimers for Surface-Enhanced Raman Spectroscopy. *J. Am. Chem. Soc.* **2010**, *132*, 10903−10910.
(3) Fan, M.; Brolo, A. G. Silver nanoparticles self assembly as SERS substrates with near single molecule detection limit. *Phys. Chem. Chem. Phys.* **2009**, *11*, 7381−7389.
(4) Nie, S.; Emory, S. R. Probing Single Molecules and Single Nanoparticles by Surface-Enhanced Raman Scattering. *Science* **1997**, *275*, 1102−1106.
(5) Talley, C. E.; Jackson, J. B.; Oubre, C.; Grady, N. K.; Hollars, C. W.; Lane, S. M.; Huser, T. R.; Nordlander, P.; Halas, N. J. Surface-Enhanced Raman Scattering from Individual Au Nanoparticles and Nanoparticle Dimer Substrates. *Nano Lett.* **2005**, *5*, 1569−1574.
(6) Liang, H.; Li, Z.; Wang, Z.; Wang, W.; Rosei, F.; Ma, D.; Xu, H. Enormous Surface-Enhanced Raman Scattering from Dimers of Flower-Like Silver Mesoparticles. *Small* **2012**, *8*, 3400−3405.
(7) Pazos-Perez, N.; Wagner, C. S.; Romo-Herrera, J. M.; Liz-Marzán, L. M.; García de Abajo, F. J.; Wittemann, A.; Fery, A.; Alvarez-Puebla, R. A. Organized Plasmonic Clusters with High Coordination Number and Extraordinary Enhancement in Surface-Enhanced Raman Scattering (SERS). *Angew. Chem., Int. Ed.* **2012**, *51*, 12688−12693.
(8) Chen, G.; Wang, Y.; Yang, M.; Xu, J.; Goh, S. J.; Pan, M.; Chen, H. Measuring Ensemble-Averaged Surface-Enhanced Raman Scattering in the Hotspots of Colloidal Nanoparticle Dimers and Trimers. *J. Am. Chem. Soc.* **2010**, *132*, 3644−3645.
(9) Schwartzberg, A. M.; Grant, C. D.; Wolcott, A.; Talley, C. E.; Huser, T. R.; Bogomolni, R.; Zhang, J. Z. Unique Gold Nanoparticle Aggregates as a Highly Active Surface-Enhanced Raman Scattering Substrate. *J. Phys. Chem. B* **2004**, *108*, 19191−19197.
(10) Lim, D.-K.; Jeon, K.-S.; Kim, H. M.; Nam, J.-M.; Suh, Y. D. Nanogap-engineerable Raman-active nanodumbbells for single-molecule detection. *Nat. Mater.* **2010**, *9*, 60−67.
(11) Qin, L.; Zou, S.; Xue, C.; Atkinson, A.; Schatz, G. C.; Mirkin, C. A. Designing, fabricating, and imaging Raman hot spots. *Proc. Natl. Acad. Sci. U. S. A.* **2006**, *103*, 13300−13303.
(12) Lee, S. Y.; Hung, L.; Lang, G. S.; Cornett, J. E.; Mayergoyz, I. D.; Rabin, O. Dispersion in the SERS Enhancement with Silver Nanocube Dimers. *ACS Nano* **2010**, *4*, 5763−5772.
(13) Qian, Z.; Hastings, S. P.; Li, C.; Edward, B.; McGinn, C. K.; Engheta, N.; Fakhraai, Z.; Park, S.-J. Raspberry-like Metamolecules Exhibiting Strong Magnetic Resonances. *ACS Nano* **2015**, *9*, 1263−1270.
(14) Joo, T. H.; Kim, M. S.; Kim, K. Surface-enhanced Raman scattering of benzenethiol in silver sol. *J. Raman Spectrosc.* **1987**, *18*, 57−60.
(15) Kleinman, S. L.; Frontiera, R. R.; Henry, A.-I.; Dieringer, J. A.; Van Duyne, R. P. Creating, characterizing, and controlling chemistry with SERS hot spots. *Phys. Chem. Chem. Phys.* **2013**, *15*, 21−36.
(16) Lim, D.-K.; Jeon, K.-S.; Hwang, J.-H.; Kim, H.; Kwon, S.; Suh, Y. D.; Nam, J.-M. Highly uniform and reproducible surface-enhanced Raman scattering from DNA-tailorable nanoparticles with 1-nm interior gap. *Nat. Nanotechnol.* **2011**, *6*, 452−460.
(17) Sanchez-Gaytan, B. L.; Swanglap, P.; Lamkin, T. J.; Hickey, R. J.; Fakhraai, Z.; Link, S.; Park, S.-J. Spiky Gold Nanoshells: Synthesis and Enhanced Scattering Properties. *J. Phys. Chem. C* **2012**, *116*, 10318−10324.
(18) Kleinman, S. L.; Sharma, B.; Blaber, M. G.; Henry, A.-I.; Valley, N.; Freeman, R. G.; Natan, M. J.; Schatz, G. C.; Van Duyne, R. P. Structure Enhancement Factor Relationships in Single Gold Nanoantennas by Surface-Enhanced Raman Excitation Spectroscopy. *J. Am. Chem. Soc.* **2013**, *135*, 301−308.
(19) Stewart, A. F.; Lee, A.; Ahmed, A.; Ip, S.; Kumacheva, E.; Walker, G. C. Rational Design for the Controlled Aggregation of Gold Nanorods via Phospholipid Encapsulation for Enhanced Raman Scattering. *ACS Nano* **2014**, *8*, 5462−5467.
(20) Jain, P. K.; El-Sayed, M. A. Plasmonic coupling in noble metal nanostructures. *Chem. Phys. Lett.* **2010**, *487*, 153−164.
(21) Oubre, C.; Nordlander, P. Finite-difference Time-domain Studies of the Optical Properties of Nanoshell Dimers. *J. Phys. Chem. B* **2005**, *109*, 10042−10051.

DOI: 10.1021/acs.jpcc.5b09396
J. Phys. Chem. C XXXX, XXX, XXX−XXX